Enterocyte Expression of Interleukin 7 Induces Development of γδ T Cells and Peyer's Patches

By Karen Laky,* Leo Lefrançois,* Elizabeth G. Lingenheld,* Hiromichi Ishikawa,‡ Julia M. Lewis,§ Sara Olson,* Kenji Suzuki,‡ Robert E. Tigelaar,§ and Lynn Puddington*

*From the *Department of Medicine, University of Connecticut Health Center, Farmington, Connecticut 06030-1310; the ‡Department of Microbiology, Keio University School of Medicine, Tokyo 160-8582, Japan; and the §Department of Dermatology, Yale University School of Medicine, New Haven, Connecticut 06520-8059*

Abstract

The intestinal mucosa is suggested to support extrathymic T cell development, particularly for T cell receptor (TCR)-γδ intraepithelial lymphocytes (IELs). TCR-γδ cell development requires interleukin (IL)-7; IL-7$^{-/-}$ or IL-7 receptor$^{-/-}$ mice lack TCR-γδ cells. Using the intestinal fatty acid binding protein (iFABP) promoter, we reinstated expression of IL-7 to mature enterocytes of IL-7$^{-/-}$ mice (iFABP-IL7). In iFABP-IL7 mice, TCR-γδ IELs were restored, as were cryptopatches and Peyer's patches. TCR-γδ cells remained absent from all other tissues. Likewise, T cell development in thymus and B cell maturation in the bone marrow and spleen retained the IL-7$^{-/-}$ phenotype. Thus, IL-7 expression by enterocytes was sufficient for extrathymic development of TCR-γδ cells in situ within the intestinal epithelium and was crucial for organization of mucosal lymphoid tissue.

Key words: immunology • cell differentiation • morphogenesis • germinal center

Introduction

The concept of extrathymic T lymphocyte development predicts that T cell progenitors and all factors required for their maturation are present at extrathymic sites. One factor known to be requisite for development of TCR-γδ cells is the cytokine IL-7. In mice lacking IL-7, IL-7 receptor (IL-7Rα or γ_c chain), or the γ_c signal transduction molecule Janus kinase (JAK)3, neither thymic nor extrathymic TCR-γδ cells are produced (1–6). The intestinal mucosa has been suggested to support extrathymic T cell development, particularly for TCR-γδ intraepithelial lymphocytes (IELs)[1] (7–13). This hypothesis is supported by demonstrations that intestinal epithelial cells express stem cell factor (SCF) (14, 15) and IL-7 (16–18), cytokines that together are essential for intrathymic T cell development (19). Moreover, anatomical structures in the intestinal mucosa, termed cryptopatches, have been described that contain T-committed lymphocyte precursors expressing the receptors for SCF (c-Kit, CD117) and IL-7 (IL-7Rα, CD127) (20). Transplantation of cryptopatch cells from *nu/nu* mice into SCID recipients generates small numbers of TCR-γδ IELs and TCR-αβ cells in the IEL and mesenteric lymph node compartments (21). However, since cryptopatches were transplanted to euthymic mice, it remains unclear whether the progeny of cryptopatch cells were derived via a bona fide process of extrathymic T cell development.

We have recently shown that extrathymic IL-7 expression is sufficient to promote development of TCR-γδ IELs in thymectomized, irradiated, bone marrow–reconstituted (ATxBM) chimeric mice (6). However, in that model system (and all other models of extrathymic T cell development), IL-7 is produced at sites other than the intestinal epithelium, most notably in the bone marrow (22), a known lymphopoietic organ. For this reason, it has been impossible to unequivocally identify the site of extrathymic TCR-γδ cell development. To circumvent this problem, we restored IL-7 expression to the intestinal epithelium of IL-7$^{-/-}$ mice using the tissue-specific intestinal fatty acid binding protein (iFABP) promoter. This model has allowed us to isolate the functional consequences of IL-7 production

Address correspondence to Lynn Puddington, Dept. of Medicine, MC-1310, University of Connecticut Health Center, 263 Farmington Ave., Farmington, CT 06030. Phone: 860-679-4655; Fax: 860-679-1287; E-mail: lpudding@panda.uchc.edu

[1]*Abbreviations used in this paper:* DETC, dendritic epidermal T cell; IELs, intraepithelial lymphocytes; iFABP, intestinal fatty acid binding protein; LP, lamina propria; PNA, peanut agglutinin; SCF, stem cell factor.

by intestinal epithelial cells from those that would normally occur in concert with IL-7–mediated hematopoiesis at other sites. Profound changes in intestinal T and B lymphocytes were induced by the IL-7 produced in the intestine, including restoration of TCR-γδ IELs and augmentation of cryptopatch and Peyer's patch assembly. These findings support the concept that a subset of TCR-γδ IELs develops completely within the intestines of normal mice. In addition, it is likely that intestine-produced IL-7 is involved in the recruitment or proliferation of lymphoid progenitors that establish the pattern of cryptopatch and Peyer's patch formation.

Materials and Methods

Generation of iFABP-IL7 Transgenic Mice. A plasmid containing the cDNA encoding IL-7 (reference 23; obtained from R. Murray and U. von Freeden-Jeffry, DNAX Research Institute of Cellular and Molecular Biology, Palo Alto, CA) was digested with XhoI. The 0.5-kb fragment containing the IL-7 cDNA was purified and BamHI sites introduced into the 5′ and 3′ ends by PCR using Taq DNA polymerase (Life Technologies). The sense primer was 5′-GGGGGATCCATGTTCCATGTTTCTTTTAGA-3′, and the antisense primer was 5′-GGGGGATCCTTATATACTGCCCTTCAAAAT-3′, obtained from Life Technologies. The correct PCR product was resolved by PAGE, and the ends of the DNA were filled in using the Klenow fragment of DNA polymerase (Roche Molecular Biochemicals). BamHI-restricted IL-7 cDNA (nucleotides 548 to 1,012; reference 23) was ligated into the expression vector, pIH, that had been linearized with BamHI. The plasmid contained the bacterial origin of replication and *amp*^{r} genes from the 2.9-kb SalI fragment derived from pSG5 (Stratagene, Inc.), the iFABP promoter (nucleotides −1178 to +28; a gift of J.I. Gordon, Washington University School of Medicine, St. Louis, MO; references 24 and 25), and hGH (nucleotides 498 to 2,652; a gift of R.M. Perlmutter, University of Washington, Seattle, WA; reference 26). The orientation of the cDNA and its complete sequence as well as the sequences of the eukaryotic control elements were verified. The SalI linear 3.9-kb fragment of pIH-IL7 was purified and microinjected into fertilized eggs obtained from IL-7$^{-/-}$ mice. IL-7$^{-/-}$ mice were originally obtained from R. Murray and U. von Freeden-Jeffry and were maintained on a C57BL/6J × 129 Ola hybrid background, as previously described (27). All mice were fed sterile food and water and were housed in microisolators under specific pathogen–free conditions. Their welfare was in accordance with institutional and Office of Laboratory Animal Welfare guidelines.

Southern Blotting. Screening of iFABP-IL7 transgenic mice was by Southern blot. Approximately 10 μg of genomic DNA (prepared from 0.25 inch of tail) was digested with PstI (Life Technologies) and electrophoresed in a 0.8% Seakem® Gold agarose gel (FMC Bioproducts). The DNA was transferred by capillary action to a NYTRAN® membrane (0.45 μm, net neutral charge; Schleicher & Schuell, Inc.) in 10× SSPE (1.5 M NaCl, 100 mM NaH_2PO_4, 12.5 mM EDTA, pH 7.4). DNA was UV cross-linked to the membrane (2,400 J) and incubated at 45°C with a probe containing the last 1,300 bp of hGH in 5 ml of hybridization buffer (0.1 M Tris-HCl, 5 mM EDTA, 0.5 mg/ml heparin, 0.1% sodium pyrophosphate, 0.5% sarcosyl, 10% dextran sulfate, 1 M NaCl, 30% formamide, and 0.1 mg/ml sheared salmon sperm, pH 7.5). DNA (~25 ng) was labeled with α-[^{32}P]dATP (Amersham Life Science) using a Random Primers DNA Labeling System (Life Technologies). Excess, unincorporated α-[^{32}P]dATP was removed by filtration through a G-50 Sephadex Quick Spin column (Boehringer Mannheim). The specific activity of the probe was 1–3 × 10^9 counts per minute per microgram.

In some cases, mice were screened by dot blot instead of Southern blot. In those cases, ~10 μg of genomic DNA was denatured in 0.3 M NaOH at 65°C for ~1.5 h. NaOH was neutralized by adding an equal volume of 12× SSC, and then serial twofold dilutions of the DNA were blotted to a NYTRAN® membrane using a MilliBlot-D dot blotting system (Millipore Corp.). Membranes were UV cross-linked and hybridized using the hGH probe as described above.

All blots were washed in 2× SSC for 15 min at room temperature, followed by one 30-min and then one 20-min wash in 0.1× SSC + 0.2% SDS at 65°C. Bands were visualized by exposing membranes to Biomax MS film (Eastman Kodak Co.) for >5 h with a BioMax TranScreen-HE intensifying screen (Eastman Kodak Co.).

RNase Protection. Entire organs were used to obtain tissue for preparation of RNA. For example, the entire thymus or intestine (duodenum, jejunum, or ileum [24]) was frozen in liquid nitrogen and pulverized to a powder (using a Bessman tissue pulverizer; Fisher Scientific). Bone marrow was aspirated using a 26-gauge needle and subjected to centrifugation to concentrate cell aggregates. RNA was isolated from powdered tissues or bone marrow plugs using guanidinium isothiocyanate and cesium chloride gradient centrifugation (28). Typically, 20 μg of RNA from each tissue was used for RNase protection experiments using a RiboQuant® multiprobe RNase protection assay system and the mCK-4 template set (PharMingen). RNA (2.5 μg) purified from T220 cells (3T3 cell line stably transfected with the IL-7 cDNA [29]; provided by H.H. Wortis, Tufts University School of Medicine, Boston, MA) served as the positive control for mRNA encoding IL-7 and SCF in RNase protection experiments.

Lymphocyte Isolation. Lymphocytes were isolated from thymi, spleens, lymph nodes, and Peyer's patches using a glass homogenizer and then passed through 100-μm NITEX nylon mesh (Tetko) to remove connective tissue. Splenic RBCs were lysed via two sequential incubations in Tris-ammonium chloride (13 mM Tris, 135 mM NH_4Cl, pH 7.2) for 4 min at 37°C. Before staining for flow cytometric analyses, splenocyte FcRs were preblocked with affinity-purified mouse IgG (200 μg/ml; Jackson ImmunoResearch Labs., Inc.).

IELs were isolated from the small intestine (gastroduodenal junction to the ileocecal junction) essentially as previously described (30). In brief, intestines were cut longitudinally and then into 5-mm pieces and washed twice with CMF (Ca^{2+}, Mg^{2+}-free HBSS with 1 mM Hepes, 2.5 mM $NaHCO_3$, pH 7.3) containing 2% FCS. Washed intestinal pieces were combined and stirred at 37°C for 20 min in CMF containing 10% FCS and 1 mM dithioerythritol (Calbiochem Corp.). This step was repeated, and the cells in the supernatants from both treatments were combined and rapidly filtered through scrubbed nylon wool (NEN™). Cells were then subjected to centrifugation on a 44/67.5% Percoll (Pharmacia) gradient. Viable cells at the interface were collected and prepared for flow cytometric analyses.

Lamina propria (LP) lymphocytes were isolated using a modified version of the protocols published by Poussier et al. (12) and Kramer and Cebra (31). After IEL isolation, the remaining epithelial cells were removed by stirring the intestinal pieces in 1.3 mM EDTA in Ca^{2+}, Mg^{2+}-free HBSS at 37°C for 30 min. This

was repeated, and both supernatants were discarded. Gut pieces were then stirred in RPMI 1640 media containing 5% FCS at 22°C for 20 min until clear, and any released cells were discarded. The complete integrity of the villi and crypts and the absence of epithelial cells at this stage of the cell isolation was confirmed histologically. After this, LP lymphocytes were released from the tissue by digestion with 100 U/ml collagenase (Life Technologies) in RPMI supplemented with 1 mM $CaCl_2$, 1 mM $MgCl_2$, and 5% FCS at 37°C for 30 min. Collagenase treatment was repeated. Cells released after each treatment were combined, washed in PBS containing 5% FCS, and then subjected to Percoll fractionation as described above for isolation of IELs.

Visualization of Dendritic Epidermal T Cells. Dendritic epidermal T cell (DETC) sheets were isolated for whole mount staining as previously described (32, 33). In brief, abdominal and back skin was shaven with a straight razor and then cut into 2.5-cm^2 pieces. Pieces were incubated for 2–4 h in EDTA buffer (116 mM NaCl, 2.6 mM KCl, 8 mM Na_2HPO_4, 1.4 mM KH_2PO_4, 20 mM EDTA, pH 7.3) in a 5% CO_2 incubator at 37°C. The epidermis was then peeled off of each piece using fine forceps. Epidermal sheets were fixed in 23°C acetone for 20 min and then washed three times in PBS on ice for a total of 30 min. Fixed sheets were incubated overnight at 4°C with biotinylated anti-CD3ε (34) diluted in PBS + 0.2% Tween 20 and then washed three times in PBS–Tween for a total of 1.5 h. Biotinylated mAbs were visualized by incubating stained sheets with streptavidin–Texas Red (Jackson ImmunoResearch Labs., Inc.) for 1 h at 37°C, followed by three washes in 1× PBS–Tween as above. Stained epidermal sheets were examined and photographed using a Nikon Optiphot microscope.

mAbs. The following mAbs were used: anti-CD3ε–FITC (145-2C11; reference 34) or anti-CD3ε–biotin (500A2); anti-TCR-γδ–PE or –biotin (GL3; reference 35); anti-TCR-γδ (3A10; reference 36); anti-TCRVγ5 (GL1; reference 35); anti-Vγ2–FITC or –biotin (UC3-10A6); anti-TCRVγ1 (2.11), a gift from P. Pereira (Institut Pasteur, Paris, France) (37); anti-TCRVδ4–FITC (GL2; reference 35); anti-TCRαβ–FITC, –Cy-Chrome, or –PE (H57.597); anti-B220 (RA3-6B2)–Cy-Chrome; anti-IgM–FITC or –biotin (Kirkegaard & Perry Labs.); unconjugated anti-IgD or anti-IgD–FITC; anti-IgA–biotin (Kirkegaard & Perry Labs.); anti-CD38 (90)–PE; anti-GL7; peanut agglutinin (PNA; Vector Labs.); anti–c-Kit (ACK2; reference 38), a gift from S.-I. Nishikawa (Kyoto University, Kyoto, Japan); irrelevant rat IgG_{2b}, κ (R35–38); and rabbit anti–rat IgG–biotin (Vector Labs.). All mAbs were obtained from PharMingen unless otherwise noted. Biotin-conjugated antibodies were visualized with streptavidin–PE or –Cy5 (Jackson ImmunoResearch Labs., Inc.).

Immunofluorescence Analyses. A single-cell suspension of lymphocytes in PBS containing 0.2% BSA and 0.1% NaN_3 (PBS/BSA/NaN_3) was incubated with 100 μl of properly diluted mAb at 4°C for 15 min. After staining, cells were washed twice with PBS/BSA/NaN_3, and relative fluorescence intensities were measured by fluorescence flow cytometry using a FACSCalibur™ (Becton Dickinson). Fluorescence intensity is presented on a four-decade log scale. A minimum of 10,000 cells within the forward versus side scatter lymphocyte gate were analyzed in each sample.

Immunohistochemical Analyses. Small intestines were cut first into 1–1.5-cm pieces and then slit open longitudinally along the mesenteric side. Intestinal pieces were placed villus side up, and a square of filter paper was placed on top. The intestine and filter paper were placed into a no. 3 cryodish (EXCEL BRAND) filter paper side up and then covered with O.C.T. freezing media (Tissue Tek; Miles, Inc.). The entire dish was then submerged in hexane that had been chilled to −70°C in a dry ice/acetone bath. Specimens were stored at −80°C until sectioning.

Intestines were cut into 5-μm-thick sections with a cryostat, placed on poly-l-lysine glass slides, and allowed to air dry. Slides were stored at −20°C until staining. Just before staining, sections were fixed in acetone. For cryptopatch staining, intestinal sections were incubated with Block-ase (Dainippon Pharmaceutical Co., Ltd.) for 10 min at 37°C to block nonspecific binding sites. All sections were incubated with properly diluted primary antibody for 30 min and then washed three times with PBS. Sections were then incubated with biotinylated goat anti–rat IgG (Cedarlane Labs.), biotinylated rabbit anti–rat IgG (Vector Labs.), or biotinylated goat anti–hamster IgG (Vector Labs.) and then washed three times with PBS. Sections were then incubated with avidin–biotin peroxidase complexes (Vectastain ABC kit; Vector Labs.). Antibodies were visualized by Vectastain DAB (3,3′-diaminobenzidine) substrate kit (Vector Labs.) according to manufacturer's instructions.

Statistical Analyses. All analyses were two-tailed Student's *t* tests conducted using InStat Instant Biostatistics (GraphPad Software).

Results

Restoration of Typical TCR-γδ IEL IL-7$^{-/-}$ Mice by an iFABP-IL7 Transgene. Four lines of IL-7$^{-/-}$ mice containing IL-7 cDNA driven by the iFABP promoter were established (iFABP-IL7). The iFABP promoter directs constitutive expression of transgenes to mature villus-associated enterocytes but not to crypt epithelial cells beginning at ∼E16 and continuing throughout life. In addition, the iFABP promoter regulates mRNA and protein expression along the longitudinal axis of the intestine, with highest levels in the jejunum and ileum and lower levels in the duodenum and proximal colon (24, 25). The pattern of expression of the IL-7 transgene in iFABP-IL7 mice was demonstrated by RNase protection (Fig. 1). As expected, IL-7 mRNA was detected in the bone marrow, thymi, and small intestines of IL-7$^{+/+}$ mice, albeit at different levels, and was absent from all tissues in IL-7$^{-/-}$ mice. In iFABP-IL7 mice, IL-7 mRNA was present in the small intestine but not in the bone marrow or thymus. Similar to other transgenes expressed using this promoter system, the highest levels of IL-7 mRNA were present in the jejunum and ileum, with lower levels in the duodenums of transgenic mice (Fig. 1, right panel). This was true for both lines of iFABP-IL7 mice tested. The amount of IL-7 mRNA present in iFABP-IL7 intestine resembled the amount of IL-7 mRNA present in the intestines of IL-7$^{+/+}$ mice, both being much lower than the amount present in the thymi of control IL-7$^{+/+}$ mice. Also notable was that the levels of mRNA encoding SCF were characteristic for each tissue examined and unaffected by the levels of mRNA encoding IL-7. The appearance of iFABP-IL7 transgenic mice was indistinguishable from their nontransgenic littermates, with no evidence of runting, alopecia, or rectal prolapse. This was in contrast to other lines of IL-7 transgenic mice, which overexpress IL-7 in wild-type IL-7$^{+/+}$ mice (17, 39). Thus, the iFABP-IL7 transgene approximated normal IL-7 production within the intestine.

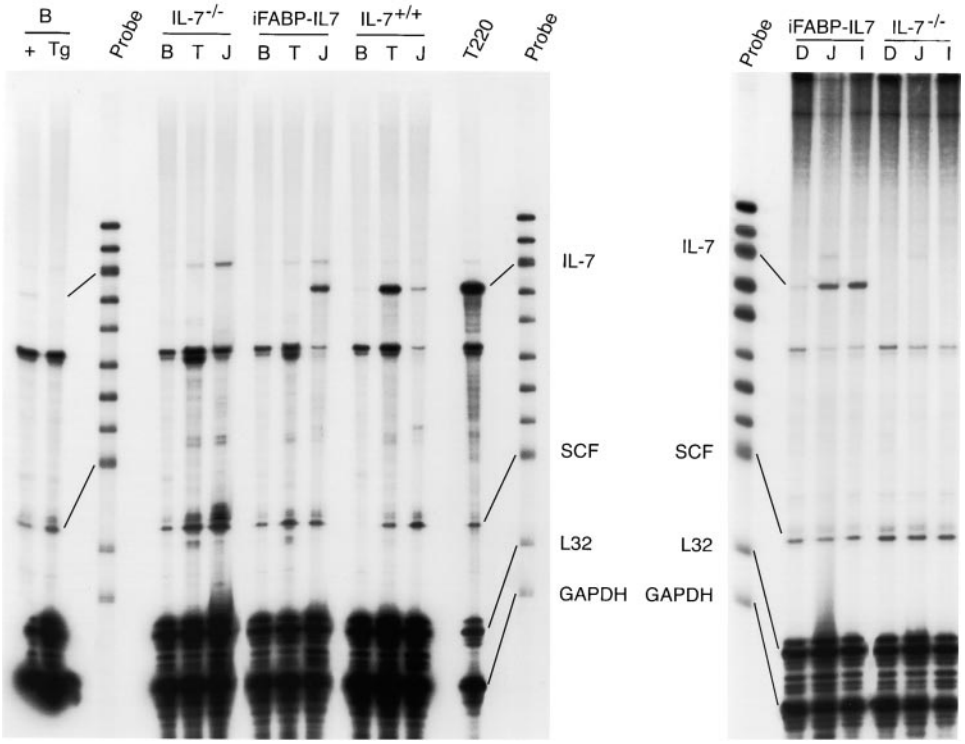

Figure 1. Pattern of expression of IL-7 mRNA in iFABP-IL7 mice. RNase protection analysis of expression of IL-7 mRNA in transgenic and nontransgenic mice. RNA was prepared from the entire organs of the tissues indicated. 20 μg of RNA from each tissue was used for RNase protection experiments using a RiboQuant® multiprobe RNase protection assay system and the mCK-4 template set (PharMingen). RNA purified from T220 cells (2.5 μg) served as the positive control for mRNA encoding IL-7 and SCF. Left panel: note the presence of IL-7 mRNA in the jejunum (J) of the intestine, but not in the bone marrow (B) or thymus (T) of iFABP-IL7 mice. IL-7 mRNA was absent from all tissues in IL-$7^{-/-}$ mice. Two far left lanes represent mRNA protected in 40 μg of bone marrow (B) RNA from wild-type (+) or iFABP-IL7 (Tg) mice. The pattern of expression of mRNA was representative of three to five individual mice analyzed for each genotype. Right panel: the expression of IL-7 mRNA in the intestine of transgenic mice was concentrated in the jejunum (J) and ileum (I), with lower levels of expression in the duodenum (D). Expression of endogenous SCF was uniform throughout the length of the intestine and irrespective of expression of IL-7.

As previously reported (2), small intestinal TCR-γδ IELs are absent from nontransgenic littermate control IL-$7^{-/-}$ mice. In contrast, expression of IL-7 under control of the iFABP promoter induced development of TCR-γδ IELs localized in the small intestinal epithelium, as demonstrated by immunohistochemistry and fluorescence flow cytometric analysis of lymphocytes after isolation (Fig. 2, A and B). The percentage and number of TCR-γδ IELs in transgenic mice was consistently less than that of age-matched IL-$7^{+/+}$ mice, ranging from 4 to 19% of $CD3^+$ small intestinal IELs as compared with 18 to 32% in wild-type mice. Similar results were obtained in two other lines of iFABP-IL7 transgenic mice (data not shown).

TCR-γδ IELs present in iFABP-IL7 mice appeared developmentally normal based on phenotypic analysis. The pattern of TCR expression was characterized on TCR-γδ IELs (Fig. 2 C). The majority of TCR-γδ cells in iFABP-IL7 mice expressed TCRVγ5, TCRVδ4, or TCRVγ1, prominent V regions of small intestine IELs expressed by normal mice, including the IL-$7^{+/+}$ line of control mice (references 30, 37, 40, 41, and data not shown). TCR-γδ IELs were also uniformly $CD8\alpha^+$ and expressed high levels of the mucosal integrin α_E (data not shown).

Restoration of Cryptopatches by an iFABP-IL7 Transgene. Cryptopatches are tiny clusters of ~1,000 c-Kit^+IL-$7R^+$Thy-$1^+$$Lineage^-$ cells located in the LP of the murine small intestine (20, 21). Cryptopatches, a potential source of extrathymic IEL precursors, are severely reduced in IL-$7R\alpha^{-/-}$ mice (20), suggesting that their formation is dependent on IL-7. The presence of cryptopatches in IL-$7^{-/-}$ mice had not been evaluated. Therefore, we looked for cryptopatches in IL-$7^{+/+}$, IL-$7^{-/-}$, and iFABP-IL7 mice (Fig. 3). Similar to other strains of mice, IL-$7^{+/+}$ mice (C57BL/6 × 129 Ola hybrid background) had ~1,500 large clusters of c-Kit^+ cells along the length of the small intestine. In contrast, the small intestines of IL-$7^{-/-}$ mice had only ~30 very small clusters of c-Kit^+ cells. This was consistent with the paucity of cryptopatches in IL-$7R\alpha^{-/-}$ mice and reemphasized the importance of IL-7 signaling in cryptopatch formation. The small intestines of iFABP-IL7 mice had ~750 cryptopatches of intermediate size. The reduced level of cryptopatches and TCR-γδ cells may be due to the fact that the iFABP promoter directs transgene expression to mature enterocytes and not crypt epithelial cells (25). Thus, the local concentration of IL-7 in iFABP-IL7 cryptopatches would be less than in wild-type mice, in which IL-7 is thought to also be expressed by crypt epithelial cells (42). Therefore, in iFABP-IL7 mice, the level of restoration of cryptopatches correlates with the level of TCR-γδ IEL production.

Restoration of Lymphocyte Development Exclusively in the Intestine in iFABP-IL7 Mice. Interestingly, in the intestinal

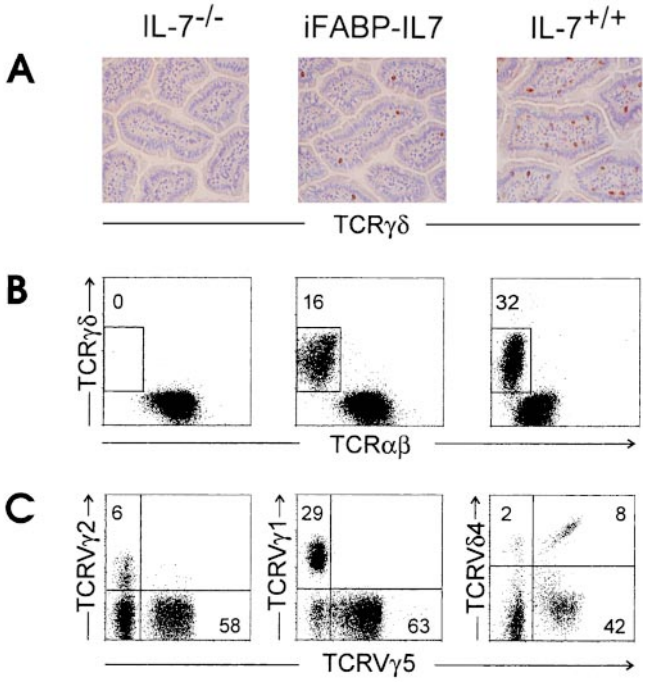

Figure 2. Restoration of typical TCR-γδ IELs in iFABP-IL7 mice. (A) Frozen sections of small intestinal villi from IL-$7^{-/-}$ (left), iFABP-IL7 (center), and IL-$7^{+/+}$ (right) mice were stained with mAb specific for TCR-γδ as described in Materials and Methods. Note the complete absence of TCR-γδ cells from IL-$7^{-/-}$ mice and partial restoration of TCR-γδ cells to iFABP-IL7 mice. (B) Small intestinal IELs were isolated from IL-$7^{-/-}$, iFABP-IL7, or age-matched IL-$7^{+/+}$ control animals. The cells were stained with mAb directed against CD3ε, TCR-αβ, and TCR-γδ and then analyzed by fluorescence flow cytometry. $CD3\epsilon^+$ cells within the forward versus side scatter lymphocyte gate were analyzed for TCR expression. The numbers indicate the percentage of TCR-$\gamma\delta^+$ cells among total $CD3\epsilon^+$ cells. (C) Small intestinal IELs from iFABP-IL7 mice were stained with mAb directed against either TCR-γδ, TCRVγ5, and TCRVγ2 or TCRVγ1 or CD3ε, TCR-αβ, TCRVγ5, and TCRVδ4. The numbers reflect the percentage of the indicated TCRVγ^+ cells among total TCR-γδ cells. Since antibodies directed against all TCR-γδ and TCRVδ4 compete for binding, $CD3\epsilon^+TCR\alpha\beta^-$ IELs were positively gated and analyzed for expression of TCRVγ5 and TCRVδ4.

mucosa of iFABP-IL7 mice, TCR-γδ cell development was restricted to the epithelium. Although a detectable population of TCR-γδ cells was present in the LP of the small intestines of IL-$7^{+/+}$ mice, no TCR-γδ cells were found in the LP of IL-$7^{-/-}$ mice or of iFABP-IL7 transgenic mice (Fig. 4 A). This result indicated that the IL-7 produced by villus enterocytes was unable to direct TCR-γδ cell development in the LP, either due to a deficiency in T cell precursors able to mature within that site or to the limited range of cytokine action. Moreover, transgenic expression of IL-7 did not restore thymic or splenic TCR-γδ cell populations (Fig. 4 A), nor did iFABP-IL7 restore normal TCR-αβ thymocyte development. Compared with IL-$7^{+/+}$ mice, the number of total thymocytes and splenic T cells in IL-$7^{-/-}$ animals are reduced 40- and 20-fold, respectively (27). These values were unaffected by the presence of the iFABP-IL7 transgene (data not shown).

Skin-resident TCR-γδ IELs (DETCs) were absent from adult iFABP-IL7 transgenic mice, as they were from IL-$7^{-/-}$ mice (Fig. 4 A). Control IL-$7^{+/+}$ mice had 404 ± 25 $CD3\epsilon^+$ DETCs per square millimeter. It is known that most, if not all, adult DETCs are the progeny of intrathymic precursors that arise during fetal life (43, 44). Therefore, since DETCs were completely absent from iFABP-IL7 mice, the existence of intestinal TCR-γδ IELs in transgenic mice cannot be the result of IL-7 production by undifferentiated epithelial cell progenitors in the embryo. Thus, when considered with the data presented in Figs. 2 and 3, iFABP-IL7 mice provide the first example of extrathymic T cell development, in situ, within the intestine.

In the absence of IL-7, the number of lymphocytes in bone marrow is greatly reduced, and the ability of B cell precursors to mature from pro- to pre-B cells is impaired (27). Unlike other IL-7 transgenic mice that overexpress IL-7 in the bone marrow (45, 46), the IL-$7^{-/-}$ bone marrow phenotype was maintained in iFABP-IL7 animals (Fig. 4 B). Bone marrow mononuclear cells from IL-$7^{-/-}$ or iFABP-IL7 mice contained $<$10% lymphocytes, compared with $>$25% in IL-$7^{+/+}$ mice. Moreover, IL-$7^{-/-}$ and iFABP-IL7 mice had reduced percentages of pre-B, immature, and mature B cells. Thus, the number of pre- and immature B cells was not elevated in iFABP-IL7 mice. This was an indication that IL-7 produced by enterocytes in the intestine had no effect on lymphopoiesis in bone marrow.

In the spleen, the absolute numbers of B cells isolated from iFABP-IL7 and nontransgenic IL-$7^{-/-}$ littermates were not different ($\sim 10^6$), and both were ~20-fold less

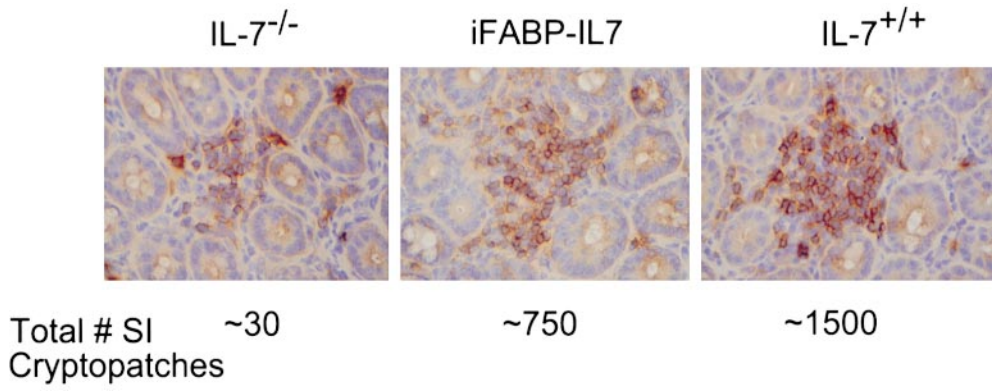

Figure 3. Restoration of cryptopatches in iFABP-IL7 mice. 6-μm frozen sections of small intestine crypts from IL-$7^{-/-}$ (left), iFABP-IL7 (center), and IL-$7^{+/+}$ (right) mice were stained with mAb specific for c-Kit as described in Materials and Methods. The cryptopatches shown typify those seen along the length of the intestine and are representative of at least three mice studied for each of the indicated genotypes. Note the intermediate number of c-Kit^+ cells in cryptopatches from iFABP-IL7 mice.

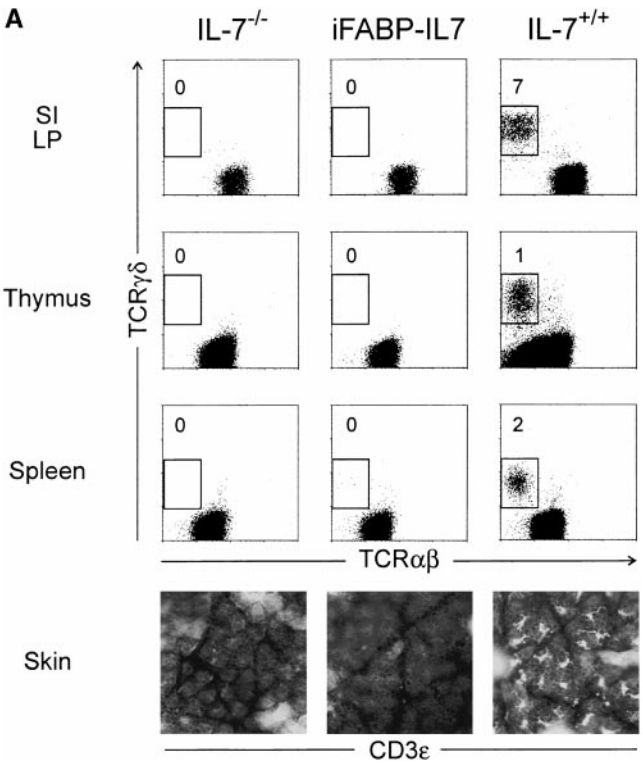

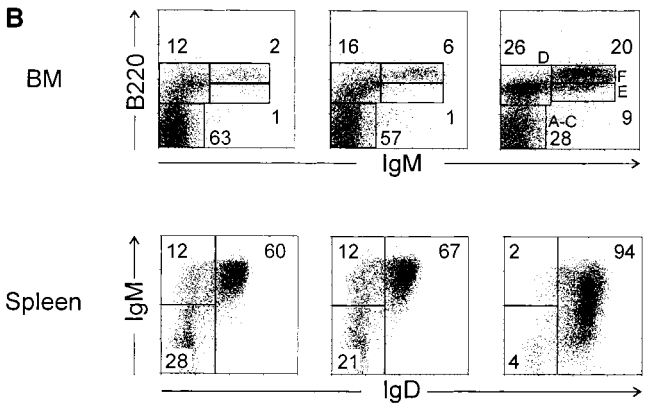

Figure 4. Intestinal epithelium–specific effects of the iFABP-IL7 transgene. (A) Lymphocytes prepared from the small intestine LP, thymus, or spleen were stained with mAb against CD3ε, TCR-αβ, and TCR-γδ. CD3ε$^+$ lymphocytes were positively gated and then analyzed for TCR-αβ and -γδ expression. The numbers indicate the percentage of TCR-γδ$^+$ cells among total CD3ε$^+$ cells. Epidermal sheets prepared from skin of 8.5-wk-old mice were stained with biotinylated anti-CD3ε, followed by streptavidin–Texas Red, and visualized by immunofluorescence microscopy. It was striking that TCR-γδ cells were restored exclusively to the intestinal epithelium of iFABP-IL7 mice and were completely absent even from small intestinal LP. (B) B cells isolated from iFABP-IL7 bone marrow or spleen were compared with B cells isolated from age-matched IL-7$^{-/-}$ or IL-7$^{+/+}$ control mice. Bone marrow cells were stained with anti-B220 and -IgM and then analyzed by fluorescence flow cytometry (top). Cells within the lymphocyte gate were analyzed to determine the relative percentages of cells within each of the B cell maturation stages defined by Hardy et al. (74). The numbers indicate the percentage of cells in each subset among total lymphocytes. Splenocytes were stained with anti-B220, -CD3, -IgM, and -IgD. CD3$^-$B220$^+$ B cells were positively gated and then analyzed for surface Ig expression (bottom). The numbers indicate the percentage of B cells in each quadrant of the phenotype indicated. No changes in the distribution of mature T (A) or B lymphocytes (B) were noted between IL-7$^{-/-}$ mice or iFABP-IL7 mice outside of the intestinal epithelium.

than that found in IL-7$^{+/+}$ mice. Moreover, the unique populations of B220$^+$IgM$^+$IgD$^-$ and B220$^+$IgM$^-$IgD$^-$ splenocytes present in IL-7$^{-/-}$ animals were maintained in transgenic mice (Fig. 4 B). The failure of the iFABP-IL7 transgene to restore normal splenic B cell populations was further evidence that the action of IL-7 was confined to the intestines of iFABP-IL7 mice. It was originally presumed that the B220$^+$IgM$^+$IgD$^-$ and B220$^+$IgM$^-$IgD$^-$ splenocytes in IL-7$^{-/-}$ animals were abnormal populations of immature B cells (27). Interestingly, our further analyses confirmed this was true only for a subset of these B lymphocytes. The B220$^+$IgM$^+$IgD$^-$ cells were a mixture of immature transi-

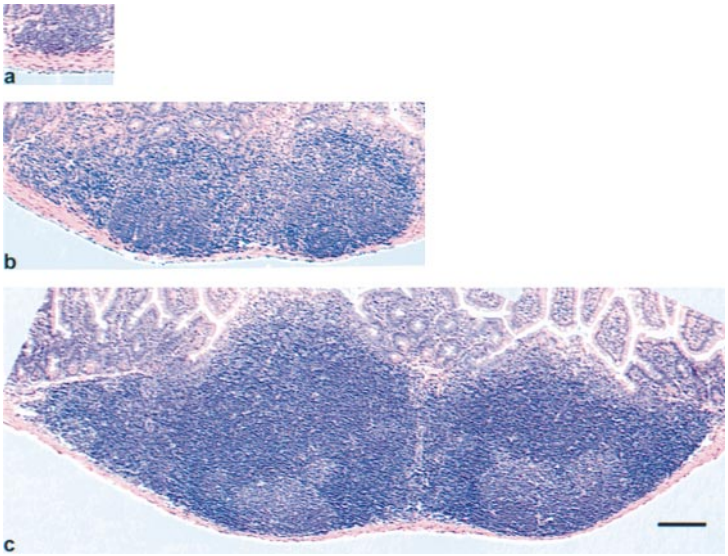

Figure 5. Restoration of Peyer's patches in iFABP-IL7 mice. Ileal Peyer's patches were dissected from the small intestines of IL-7$^{-/-}$ (a), iFABP-IL7 (b), or age-matched IL-7$^{+/+}$ control mice (c). 5-μm paraffin sections were stained with hematoxylin and eosin. Note that the small intestinal ileal Peyer's patches from iFABP-IL7 animals were larger than those of IL-7$^{-/-}$ littermates but smaller than those of age-matched IL-7$^{+/+}$ control mice. Scale bar, 100 μm.

Table I. *Regional Distribution of Small Intestinal Peyer's Patches*

Mouse	Duodenum	Jejunum	Ileum
	0, 0, 0, 0, 0, 0, 0, 0,	0, 0, 0, 0, 0, 0, 0, 0,	0, 1, 1, 2, 2, 2, 2, 2,
IL-7$^{-/-}$	0, 0, 0, 0, 0, 0, 0	0, 0, 0, 1, 1, 1, 2*	2, 2, 2, 2, 2, 3, 3*
iFABP-IL7	0, 0, 0, 0, 0	0, 1, 2, 2, 2	2, 2, 3, 3, 4
	1, 1, 1, 1, 1	2, 2, 2, 3, 4	2, 2, 3, 3, 3
IL-7$^{+/+}$	1, 1, 1, 1*	4, 4, 5, 5*	3, 4, 4, 4

Two-tailed unpaired Student's *t* tests were performed to compare the numbers of Peyer's patches in different regions of small intestine from 4–9-wk-old IL-7$^{-/-}$, iFABP-IL7, and age-matched IL-7$^{+/+}$ control mice.
*Significantly different than iFABP-IL7 transgenic animals ($P < 0.01$).

tional B cells, being CD38^{high}HSA^{high}PNA^{low}CD62L^{-}, and marginal zone B cells, being HSA^{low}CD21^{+}CD23^{-}CD1^{+} (47, 48). The absolute number of cells in each B cell subset did not exceed the numbers found in IL-7$^{+/+}$ mice (data not shown). The unique population of B220^{+}IgM^{-}IgD^{-} cells in the spleens of IL-7$^{-/-}$ mice (both transgenic and nontransgenic) contained CD38^{low}HSA^{high}PNA^{high}GL7^{+} and IgG^{+} cells visualized by flow cytometric and immunohistochemical analyses (data not shown), suggesting that impaired B cell development, in both bone marrow and the periphery of IL-7$^{-/-}$ mice, resulted in more prominent populations of germinal center and memory B cells (49).

Restoration of Peyer's Patches by an iFABP-IL7 Transgene. Macroscopic examination of the small intestines of iFABP-IL7 mice revealed a prominent effect of the transgene on Peyer's patches. In contrast to the minimal Peyer's patch development in IL-7$^{-/-}$ mice (27), there were profound increases in the size and number of Peyer's patches in transgenic mice with IL-7 produced by mature enterocytes, cells that comprise 90% of the surface area of the follicle-associated epithelium (50). Histological analyses indicated that in iFABP-IL7 mice, Peyer's patches were up to fourfold larger than those found in IL-7$^{-/-}$ mice (Fig. 5). In IL-7$^{+/+}$ mice, 6–10 Peyer's patches were found at relatively constant locations along the antimesenteric side of the small intestine, concentrated in the jejunum and ileum (Table I). Only small ileal Peyer's patches were consistently detected in IL-7$^{-/-}$ animals. In contrast, there was a significant increase in the number of visible ileal and jejunal Peyer's patches in iFABP-IL7 mice. In IL-7$^{+/+}$ mice, a single Peyer's patch was always observed in the area of the duodenal–jejunal border, and this Peyer's patch was not restored by the transgene. The regional localization of Peyer's patches in iFABP-IL7 mice paralleled the pattern of expression of IL-7 in the intestine (Fig. 1, right panel).

Peyer's Patches in iFABP-IL7 Mice Had Increased Germinal Center B Cells. Restoration of Peyer's patches in iFABP-IL7 mice was not due to increased B cell development in bone marrow (Fig. 4 B), suggesting that the effect of IL-7 on Peyer's patches occurred directly within Peyer's patches in iFABP-IL7 mice. Thus, we examined the phenotype of lymphocytes present in Peyer's patches from IL-7$^{-/-}$, iFABP-IL7, or IL-7$^{+/+}$ mice. No differences were noted in the distribution of CD4^{+} or CD8^{+} T cell subsets (data not shown). Interestingly, among Peyer's patch B lymphocytes, IL-7$^{-/-}$ and iFABP-IL7 animals had at least fivefold higher percentages of CD38^{low}IgA^{+}HSA^{high}PNA^{high}CD22^{low} cells as compared with IL-7$^{+/+}$ animals (Fig. 6 and data not shown). IL-7$^{-/-}$ and iFABP-IL7 animals also had increased percentages of CD38^{low}IgA^{+} cells in LP (data not shown). These data indicated that the ability to form germinal centers and to undergo Ig class switch recombination was not impaired in Peyer's patches in IL-7$^{-/-}$ mice.

The relative percentage of naive and germinal center B cells was altered in iFABP-IL7 mice (Fig. 6). Thus, we sought to determine whether the architecture of Peyer's patches in iFABP-IL7 mice was normal. Immunohistochemical analyses of frozen sections revealed that the overall

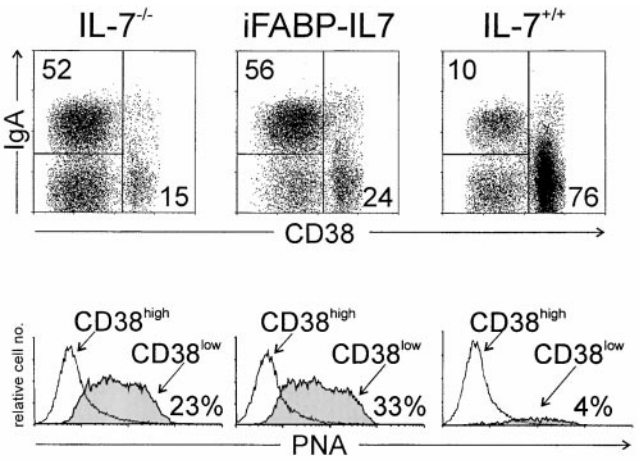

Figure 6. B lymphocyte maturation in Peyer's patches in iFABP-IL7 mice. Peyer's patch lymphocytes were prepared as described in Materials and Methods and then stained with anti-B220, -CD38, and -IgA or PNA and analyzed by flow cytometry. B220^{+} cells were positively gated and then analyzed for level of CD38 expression and cell surface IgA (top). The numbers indicate the percentage of B220^{+} cells that fell within each quadrant. The CD38^{high}IgA^{-} cells in the lower right quadrant were IgM^{+} (data not shown). B220^{+}CD38^{high} or B220^{+}CD38^{low} cells were positively gated and then analyzed for their ability to bind PNA (bottom). The percentages of PNA^{+} cells among total B220^{+} cells are indicated.

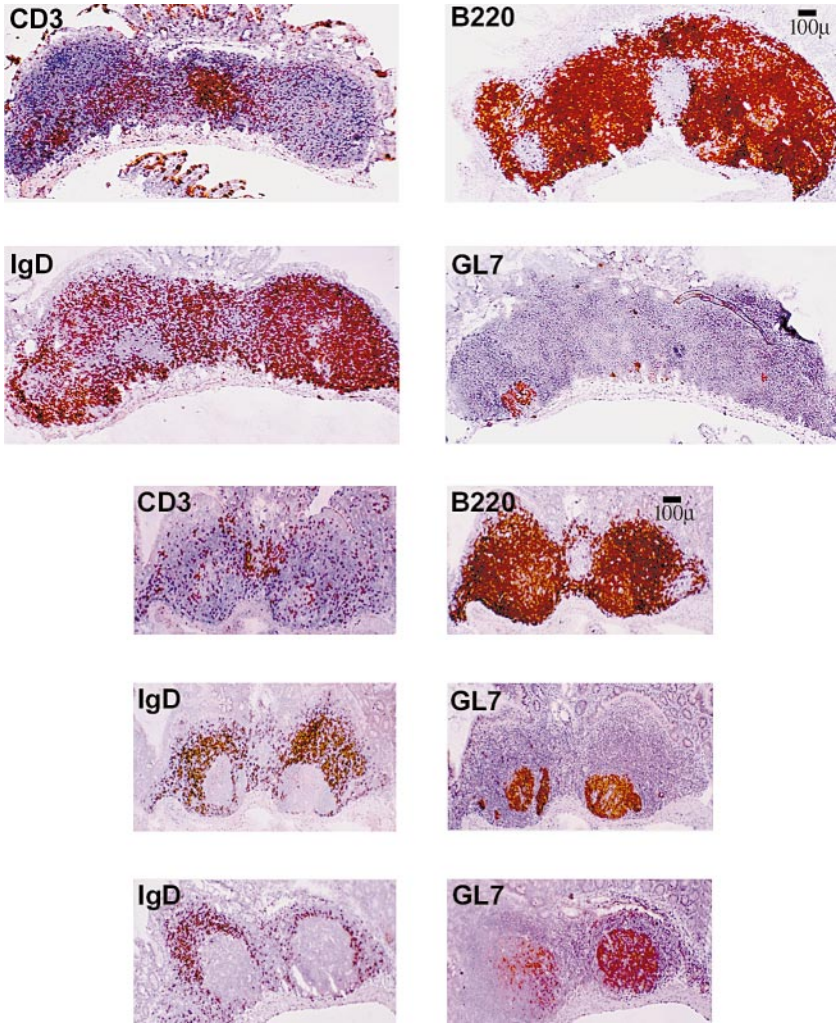

Figure 7. Visualization of germinal centers in iFABP-IL7 Peyer's patches. Peyer's patches were dissected from the small intestine of age-matched control IL-$7^{+/+}$ mice (top) or iFABP-IL7 mice (bottom). 6-μm frozen sections were stained as described in Materials and Methods with mAbs that identified total B cells ($B220^+$), total T cells ($CD3^+$), naive B cells (IgD^+), or germinal center B cells ($GL7^+$). The iFABP transgene restored germinal centers to approximately the size visualized in normal mice, despite the concurrent deficiency in naive B cells.

structure of Peyer's patches was the same in adult iFABP-IL7 and IL-$7^{+/+}$ mice (Fig. 7). The spatial distribution of T cells ($CD3^+$), B cells ($B220^+$), and marginal zone macrophages (MOMA-1^+; data not shown) did not differ between iFABP-IL7 and IL-$7^{+/+}$ mice. However, there was a striking difference in the phenotype of B lineage cells. Consistent with previous reports (49, 51), the majority of B cells in Peyer's patches from IL-$7^{+/+}$ mice were naive IgD^+ B cells. In contrast, $GL7^+$ germinal center B cells accounted for a very large percentage of total Peyer's patch volume in Peyer's patches from iFABP-IL7 mice, with far fewer IgD^+ cells. These results, taken together with the flow cytometry data presented in Fig. 6 and macroscopic observations that similar numbers of follicles were visualized in each Peyer's patch present in iFABP-IL7 mice, suggest that intestinal IL-7 promotes organogenesis of Peyer's patches in normal mice.

Discussion

Our results provide compelling evidence for extrathymic development of TCR-γδ IELs in situ, within the intestine of iFABP-IL7 animals. Intestinal epithelial cells normally express IL-7 (Fig. 1 and reference 16–18), and TCR-γδ cells were reconstituted solely within the intestinal epithelium of iFABP-IL7 IL-$7^{-/-}$ mice. Thus, iFABP-IL7 mice are an extraordinary model system for studying normal extrathymic TCR-γδ cell development in vivo, without extensive and invasive experimental manipulation, i.e., irradiation, thymectomy, or intravenous transfer of hematopoietic precursors. Because the expression and action of IL-7 in iFABP-IL7 animals was exquisitely regulated, this is the first model system that allows the extrathymic site of TCR-γδ cell development to be precisely identified. De novo generation of TCR-γδ IELs in iFABP-IL7 mice indicated that all IL-7–dependent steps of T cell development occurred within the intestine, including commitment to the TCR-γδ cell lineage. It is agreed that IL-7R signaling influences TCR-γ gene rearrangement (52–55) or expression of TCRVγ genes (56–62). Since signaling through IL-7R promotes TCR-γ gene rearrangement and/or transcription, then IL-7 produced within the intestine provided the stimulus to initiate extrathymic development of TCR-γδ cells. Also present

within the intestine were lymphoid progenitors that responded to IL-7, as well as other growth factors (e.g., SCF) required for homeostasis of mature TCR-γδ IELs.

The reduced number of TCR-γδ IELs in iFABP-IL7 mice was not surprising, as these mice lack thymus-derived mature TCR-γδ IELs, which comprise a subset of IELs in normal mice (6, 63). Moreover, IL-$7^{-/-}$ mice appear to have reduced numbers of extrathymic T cell progenitors (6, 20) that were only partially restored in iFABP-IL7 mice. In normal mice, cryptopatches are not detected until after birth, but then they are maintained throughout their lifespans. Cryptopatches are rare in IL-$7R\alpha^{-/-}$ mice (20). This suggests that cryptopatches are colonized with progenitor cells from bone marrow and then are either self-renewing or continuously replenished from IL-7–dependent hematopoiesis in bone marrow, which was not restored in iFABP-IL7 mice. Despite this, the concomitant restoration of TCR-γδ IELs and intestinal cryptopatches in iFABP-IL7 mice supports the hypothesis that cryptopatches contain extrathymic IEL precursors.

The RNase protection assay used to verify the tissue-specific expression of transgenic IL-7 allowed simultaneous visualization of multiple cytokine mRNAs. Thus, the relative amounts of growth factor mRNAs were compared within individual samples. IL-7 and SCF are two cytokines critical for normal thymic (19) and extrathymic T cell development (our unpublished results). We and others have shown that stromal cells in bone marrow, thymus, and intestine express IL-7 and SCF mRNA (14, 16, 18, 42, 64–66). However, the relative levels of these two cytokines in each lymphopoietic site had not been evaluated. The RNase protection data in Fig. 1 clearly showed that the relative levels of IL-7 and SCF mRNA were inverse in the thymus and intestine in control IL-$7^{+/+}$ mice. In the thymus, mRNA encoding IL-7 was greater than that encoding SCF, whereas in the intestine, mRNA encoding SCF was greater than that encoding IL-7. This pattern of mRNA expression was not unique to this strain of mice, as it was also observed in C57BL/6J and $WCB6F_1$ wild-type mice (data not shown). The significance of this finding to thymic and extrathymic T cell development is not yet clear. However, it is notable that most TCR-γδ thymocytes in adult mice express IL-7Rα, whereas most TCR-γδ IELs express c-Kit (6) and proliferate in response to SCF production in vivo (15).

The effect of IL-7 on Peyer's patch development further emphasized the critical role for IL-7 in ontogeny of the mucosal immune system. It has been reported that IL-7Rα and JAK3 are required for the formation of the fetal Peyer's patch anlage (67). Our data showed that in adult IL-$7^{-/-}$ mice, limited Peyer's patch formation occurred in the absence of IL-7, but transgene-directed IL-7 expression by villus enterocytes increased the number of Peyer's patches formed and increased their size. Germinal center formation in Peyer's patches was not compromised in the absence of IL-7. In fact, the opposite result was obtained whereby the fraction of B cells in germinal centers ($CD3^-B220^+CD38^{low}PNA^+GL7^+$) was increased without IL-7. Thus, the lack of active germinal centers in $\gamma_c^{-/-}$ mice cannot be attributed to the absence of IL-7R signaling (1). Compatible with this is the observation that another cytokine that utilizes the γ_c receptor, IL-4, is critical for germinal center formation in the intestinal mucosa (68).

The paucity of naive B cells (IgD^+ cells) in Peyer's patches of iFABP-IL7 mice (Fig. 7) was consistent with the IL-7 deficiency outside of the intestine, a consequence of decreased de novo development of B cells in bone marrow (27). Thus, the increased size and number of Peyer's patches in iFABP-IL7 mice suggested that IL-7 influenced B cell maturation within the intestine. IL-7 may have directly affected Peyer's patch B cells by supporting de novo B cell development within Peyer's patches, as occurs in sheep (69). Alternatively, IL-7 production by Peyer's patch follicle-associated epithelium may have facilitated entry of the small number of bone marrow–derived transitional B cells to the recirculating pool within Peyer's patches or augmented their proliferation in situ. Although it is believed that in normal mice most transitional B cells enter the recirculating pool in the spleen (47, 48, 70), asplenic *Hox11*$^{-/-}$ mice have normal B cell profiles in lymph node and peripheral blood and demonstrate robust Ig responses after immunization. This indicates that the final stages of B cell maturation can occur outside of spleen (71, 72). Indeed, the naive B cells in the Peyer's patches of iFABP-IL7 mice may represent the normal contribution of Peyer's patch–derived IL-7 to the process of B cell selection.

Another possibility was that enterocyte-produced IL-7 affected B cell development indirectly, by influencing other cell types that then affected B cells within Peyer's patches. For example, iFABP-IL7 may have augmented T helper function or IL-4 production. Alternatively, intestinal IL-7 may have enhanced the development/recruitment of IL-$7R\alpha^+$ stromal elements or lymphoid cell progenitors involved in Peyer's patch formation and structure, as occurs during assembly of the murine fetal Peyer's patch anlage (67, 73). This transgenic model is currently being exploited in experiments designed to resolve these issues. It is clear that iFABP-IL7 mice will provide a powerful tool for defining the role of IL-7 in Peyer's patch development and more generally in B cell maturation.

We thank David Masopust for assistance in preparing the DNA construct and the University of Connecticut Health Center Transgenic facility for generating transgenic mice. We are grateful for the help of Kristine Mack and Deborah Cassarino in establishing protocols for screening and analysis of tail DNA. We also thank Drs. Nyls Lycke and Brian Kelsall for helpful discussions regarding the structure of murine Peyer's patches.

This work was supported by U.S. Public Health Service Grants DK51505 (to L. Puddington), AI35917 (to L. Lefrançois and L. Puddington), and AI27404 (to R. Tigelaar); and by the Agency of Science and Technology (Japan) and Japan Society for the Promotion of Science (grant JSPS-RFTF 97L00701 to H. Ishikawa). K. Laky was supported by National Institutes of Health pre-doctoral training grant AI07080. L. Lefrançois was supported by an American Cancer Society Faculty Research Award.

Submitted: 8 December 1999
Revised: 1 February 2000
Accepted: 4 February 2000

References

1. Cao, X., E.W. Shores, J. Hu-Li, M.R. Anver, B.L. Kelsall, S.M. Russell, J. Drago, M. Noguchi, A. Grinberg, E.T. Bloom, et al. 1995. Defective lymphoid development in mice lacking expression of the common cytokine receptor γ chain. *Immunity*. 2:223–238.
2. Moore, T.A., U. von Freeden-Jeffry, R. Murray, and A. Zlotnik. 1996. Inhibition of γδ T cell development and early thymocyte maturation in IL-7$^{-/-}$ mice. *J. Immunol.* 157: 2366–2373.
3. Park, S.Y., K. Saijo, T. Takahashi, M. Osawa, H. Arase, N. Hirayama, K. Miyake, H. Nakauchi, T. Shirasawa, and T. Saito. 1995. Developmental defects of lymphoid cells in jak3 kinase-deficient mice. *Immunity*. 3:771–782.
4. He, Y.W., and T.R. Malek. 1996. Interleukin-7 receptor α is essential for the development of γδ$^+$ T cells, but not natural killer cells. *J. Exp. Med.* 184:289–293.
5. Maki, K., S. Sunaga, Y. Komagata, Y. Kodaira, A. Mabuchi, H. Karasuyama, K. Yokomuro, J.I. Miyazaki, and K. Ikuta. 1996. Interleukin 7 receptor-deficient mice lack γδ T cells. *Proc. Natl. Acad. Sci. USA*. 93:7172–7177.
6. Laky, K., L. Lefrançois, U. von Freeden-Jeffry, R. Murray, and L. Puddington. 1998. The role of IL-7 in thymic and extrathymic development of TCRγδ cells. *J. Immunol.* 161: 707–713.
7. Lefrançois, L., J. Mayo, and T. Goodman. 1990. Ontogeny of T cell receptor (TCR) α,β+ and γ,δ+ intraepithelial lymphocytes (IEL). *In* Cellular Immunity and the Immunotherapy of Cancer. M.T. Lotze and O.J. Finn, editors. Wiley-Liss, New York. 31–40.
8. Bandeira, A., S. Itohara, M. Bonneville, O. Burlen-Defranoux, T. Mota-Santos, A. Coutinho, and S. Tonegawa. 1991. Extrathymic origin of intestinal intraepithelial lymphocytes bearing T-cell antigen receptor γδ. *Proc. Natl. Acad. Sci. USA*. 88:43–47.
9. De Geus, B., M. Van den Enden, C. Coolen, L. Nagelkerken, P. Van der Heijden, and J. Rozing. 1990. Phenotype of intraepithelial lymphocytes in euthymic and athymic mice: implications for differentiation of cells bearing a CD3-associated γδ T cell receptor. *Eur. J. Immunol.* 20:291–298.
10. Rocha, B., P. Vassalli, and D. Guy-Grand. 1991. The Vβ repertoire of mouse gut homodimeric α CD8$^+$ intraepithelial T cell receptor α/β$^+$ lymphocytes reveals a major extrathymic pathway of T cell differentiation. *J. Exp. Med.* 173:483–486.
11. Whetsell, M., R.L. Mosley, L. Whetsell, F.V. Schaefer, K.S. Miller, and J.R. Klein. 1991. Rearrangement and junctional-site sequence analyses of T-cell receptor gamma genes in intestinal intraepithelial lymphocytes from murine athymic chimeras. *Mol. Cell. Biol.* 11:5902–5909.
12. Poussier, P., P. Edouard, C. Lee, M. Binnie, and M. Julius. 1992. Thymus-independent development and negative selection of T cells expressing T cell receptor α/β in the intestinal epithelium: evidence for distinct circulation patterns of gut- and thymus-derived T lymphocytes. *J. Exp. Med.* 176:187–199.
13. Lefrançois, L., and S. Olson. 1997. Reconstitution of the extrathymic intestinal T cell compartment in the absence of irradiation. *J. Immunol.* 159:538–541.
14. Puddington, L., S. Olson, and L. Lefrançois. 1994. Interactions between stem cell factor and c-Kit are required for intestinal immune system homeostasis. *Immunity*. 1:733–739.
15. Laky, K., L. Lefrançois, and L. Puddington. 1997. Age-dependent intestinal lymphoproliferative disorder due to stem cell factor receptor deficiency. *J. Immunol.* 158:1417–1427.
16. Fujihashi, K., S. Kawabata, T. Hiroi, M. Yamamoto, J.R. Mcghee, S.-I. Nishikawa, and H. Kiyono. 1996. Interleukin-2 (IL-2) and interleukin-7 (IL-7) reciprocally induce IL-7 and IL-2 receptors on γδ T cell receptor-positive intraepithelial lymphocytes. *Proc. Natl. Acad. Sci. USA*. 93:3613–3618.
17. Watanabe, M., Y. Ueno, T. Yajima, S. Okamoto, T. Hayashi, M. Yamazaki, Y. Iwao, H. Ishii, S. Habu, M. Uehira, et al. 1998. Interleukin 7 transgenic mice develop chronic colitis with decreased interleukin 7 protein accumulation in the colonic mucosa. *J. Exp. Med.* 187:389–402.
18. Murray, A.M., B. Simm, and K.W. Beagley. 1998. Cytokine gene expression in murine fetal intestine: potential for extrathymic T cell development. *Cytokine*. 10:337–345.
19. Di Santo, J.P., and H.-R. Rodewald. 1998. In vivo roles of receptor tyrosine kinases and cytokine receptors in early thymocyte development. *Curr. Opin. Immunol.* 10:197–207.
20. Kanamori, Y., K. Ishimaru, M. Nanno, K. Maki, K. Ikuta, H. Nariuchi, and H. Ishikawa. 1996. Identification of novel lymphoid tissues in murine intestinal mucosa where clusters of c-kit$^+$ IL-7R$^+$ Thy1$^+$ lympho-hemopoietic progenitors develop. *J. Exp. Med.* 184:1449–1459.
21. Saito, H., Y. Kanayama, T. Takemori, H. Nariuchi, E. Kubota, H. Takahashi-Iwanaga, T. Iwanaga, and H. Ishikawa. 1998. Generation of intestinal T cells from progenitors residing in gut cryptopatches. *Science*. 280:275–278.
22. Funk, P.E., R.P. Stephan, and P.L. Witte. 1995. Vascular cell adhesion molecule 1-positive reticular cells express interleukin-7 and stem cell factor in the bone marrow. *Blood*. 86: 2661–2671.
23. Namen, A.E., S. Lupton, K. Hjerrild, J. Wignall, D.Y. Mochizuki, A. Schmierer, B. Mosley, C.J. March, D. Urdal, S. Gillis, et al. 1988. Stimulation of B-cell progenitors by cloned murine interleukin-7. *Nature*. 333:571–573.
24. Sweetser, D.A., S.M. Hauft, P.C. Hoppe, E.H. Birkenmeier, and J.I. Gordon. 1988. Transgenic mice containing intestinal fatty acid-binding protein-human growth hormone fusion genes exhibit correct regional and cell-specific expression of the reporter gene in their small intestine. *Proc. Natl. Acad. Sci. USA*. 85:9611–9615.
25. Cohn, S.M., T.C. Simon, K.A. Roth, E.H. Birkenmeier, and J.I. Gordon. 1992. Use of transgenic mice to map cis-acting elements in the intestinal fatty acid binding protein gene (Fabpi) that control its cell lineage-specific and regional patterns of expression along the duodenal-colonic and crypt-villus axes of the gut epithelium. *J. Cell Biol.* 119:27–44.
26. Chaffin, K., C.R. Beals, T.M. Wilkie, K.A. Forbush, M.I. Simon, and R.M. Perlmutter. 1990. Dissection of thymocyte signaling pathways by in vivo expression of pertussis toxin ADP-ribosyltransferase. *EMBO (Eur. Mol. Biol. Organ.) J.* 9:3821–3829.
27. von Freeden-Jeffry, U., P. Vieira, L.A. Lucian, T. McNeil, S.E.G. Burdach, and R. Murray. 1995. Lymphopenia in interleukin (IL)-7 gene-deleted mice identifies IL-7 as a nonredundant cytokine. *J. Exp. Med.* 181:1519–1526.
28. Church, G.M., and W. Gilbert. 1984. Genomic sequencing. *Proc. Natl. Acad. Sci. USA*. 81:1991–1995.
29. Borzillo, G.V., K. Endo, and Y. Tsujimoto. 1992. Bcl-2 confers growth and survival advantage to interleukin 7-dependent early pre-B cells which become factor independent by a

multistep process in culture. *Oncogene*. 7:869–876.
30. Goodman, T., and L. Lefrançois. 1988. Expression of the γδ T-cell receptor on intestinal CD8+ intraepithelial lymphocytes. *Nature*. 333:855–858.
31. Kramer, D.R., and J.J. Cebra. 1995. Early appearance of "natural" mucosal IgA responses and germinal centers in suckling mice developing in the absence of maternal antibodies. *J. Immunol.* 154:2051–2062.
32. Mallick-Wood, C.A., J.M. Lewis, L.I. Richie, M.J. Owen, R.E. Tigelaar, and A.C. Hayday. 1998. Conservation of T cell receptor conformation in epidermal gamma delta cells with disrupted primary V gamma gene usage. *Science*. 279: 1729–1733.
33. Bergstresser, P.R., and D.V. Juarez. 1984. Detection by immunochemical techniques of cell surface markers on epidermal Langerhans cells. *Methods Enzymol.* 108:683–691.
34. Leo, O., M. Foo, D.H. Sachs, L.E. Samelson, and J.A. Bluestone. 1987. Identification of a monoclonal antibody specific for a murine T3 polypeptide. *Proc. Natl. Acad. Sci. USA*. 84: 1374–1378.
35. Goodman, T., and L. Lefrançois. 1989. Intraepithelial lymphocytes. Anatomical site, not T cell receptor form, dictates phenotype and function. *J. Exp. Med.* 170:1569–1581.
36. Itohara, S., P. Mombaerts, J. Lafaille, J. Iacomini, A. Nelson, A.R. Clarke, M.L. Hooper, A. Farr, and S. Tonegawa. 1993. T-cell receptor δ-gene mutant mice—independent generation of αβ T-cells and programmed rearrangements of γδ TCR genes. *Cell*. 72:337–348.
37. Pereira, P., D. Gerber, S.Y. Huang, and S. Tonegawa. 1995. Ontogenic development and tissue distribution of Vγ1-expressing γ/δ T lymphocytes in normal mice. *J. Exp. Med.* 182:1921–1930.
38. Okada, S., H. Nakauchi, K. Nagayoshi, S. Nishikawa, S.-I. Nishikawa, Y. Miura, and T. Suda. 1991. Enrichment and characterization of murine hematopoietic stem cells that express c-kit molecule. *Blood*. 78:1706–1712.
39. Williams, I.R., E.A. Rawson, L. Manning, T. Karaoli, B.E. Rich, and T.S. Kupper. 1997. IL-7 overexpression in transgenic mouse keratinocytes causes a lymphoproliferative skin disease dominated by intermediate TCR cells: evidence for a hierarchy in IL-7 responsiveness among cutaneous T cells. *J. Immunol.* 159:3044–3056.
40. Itohara, S., A.G. Farr, J.J. Lafaille, M. Bonneville, Y. Takagaki, W. Hass, and S. Tonegawa. 1990. Homing of a γδ thymocyte subset with homogeneous T-cell receptors to mucosal epithelia. *Nature*. 343:754–757.
41. Asarnow, D.M., T. Goodman, L. Lefrançois, and J.P. Allison. 1989. Distinct antigen receptor repertoires of two classes of murine epithelium-associated T cells. *Nature*. 341:60–62.
42. Watanabe, M., Y. Ueno, T. Yajima, Y. Iwao, M. Tsuchiya, H. Ishikawa, S. Aiso, T. Hibi, and H. Ishii. 1995. Interleukin 7 is produced by human intestinal epithelial cells and regulates the proliferation of intestinal mucosal lymphocytes. *J. Clin. Invest.* 95:2945–2953.
43. Havran, W.L., and J.P. Allison. 1990. Origin of Thy-1+ dendritic epidermal cells of adult mice from fetal thymic precursors. *Nature*. 344:68–70.
44. Ikuta, K., T. Kina, I. MacNeil, N. Uchida, B. Peault, Y. Chien, and I.L. Weissman. 1990. A developmental switch in thymic lymphocyte maturation potential occurs at the level of hematopoietic stem cells. *Cell*. 62:863–874.
45. Mertsching, E., U. Grawunder, V. Meyer, T. Rolink, and R. Ceredig. 1996. Phenotypic and functional analysis of B lymphopoiesis in interleukin-7-transgenic mice: expansion of pro/pre-B cell number and persistence of B lymphocyte development in lymph nodes and spleen. *Eur. J. Immunol.* 26: 28–33.
46. Rich, B.E., J. Campos-Torres, R.I. Tepper, R.W. Moreadith, and P. Leder. 1993. Cutaneous lymphoproliferation and lymphomas in interleukin 7 transgenic mice. *J. Exp. Med.* 177:305–316.
47. MacLennan, I. 1998. B-cell receptor regulation of peripheral B cells. *Curr. Opin. Immunol.* 10:220–225.
48. Loder, F., B. Mutschler, R.J. Ray, C.J. Paige, P. Sideras, R. Torres, M.C. Lamers, and R. Carsetti. 1999. B cell development in the spleen takes place in discrete steps and is determined by the quality of B cell receptor-derived signals. *J. Exp. Med.* 190:75–89.
49. Oliver, A.M., F. Martin, and J.F. Kearney. 1997. Mouse CD38 is down-regulated on germinal center B cells and mature plasma cells. *J. Immunol.* 158:1108–1115.
50. Kato, T., and R.L. Owen. 1994. Structure and function of intestinal mucosal epithelium. *In* Handbook of Mucosal Immunology. P.L. Ogra, J. Mestecky, M.E. Lamm, W. Strober, J.R. Mcghee, and J. Bienenstock, editors. Academic Press, Inc., San Diego, CA. 11–26.
51. Butcher, E.C., R.V. Rouse, R.L. Coffman, C.N. Nottenburg, R.R. Hardy, and I.L. Weissman. 1982. Surface phenotype of Peyer's patch germinal center cells: implications for the role of germinal centers in B cell differentiation. *J. Immunol.* 129:2698–2707.
52. Maki, K., S. Sunaga, and K. Ikuta. 1996. The V-J recombination of T cell receptor-γ genes is blocked in interleukin-7 receptor–deficient mice. *J. Exp. Med.* 184:2423–2428.
53. Candeias, S., J.J. Peschon, K. Muegge, and S.K. Durum. 1997. Defective T-cell receptor γ gene rearrangement in interleukin-7 receptor knockout mice. *Immunol. Lett.* 57:9–14.
54. Durum, S.K., S. Candeias, H. Nakajima, W.J. Leonard, A.M. Baird, L.J. Berg, and K. Muegge. 1998. Interleukin 7 receptor control of T cell receptor γ gene rearrangement: role of receptor-associated chains and locus accessibility. *J. Exp. Med.* 188:2233–2241.
55. Haks, M.C., M.A. Oosterwegel, B. Blom, H.M. Spits, and A.M. Kruisbeek. 1999. Cell-fate decisions in early T cell development: regulation by cytokine receptors and the pre-TCR. *Semin. Immunol.* 11:23–37.
56. Appasamy, P.M., Y. Weng, T.W. Kenniston, Jr., A.B. Deleo, and L. Tang. 1995. Expression of diverse and functional TCR γ and Ig heavy chain transcripts in fetal liver cells cultured with interleukin-7. *Mol. Immunol.* 32:805–817.
57. Soloff, R.S., T.-G. Wang, D. Dempsey, S.R. Jennings, R.M. Wolcott, and R. Chervenak. 1997. Interleukin 7 induces TCR gene rearrangement in adult marrow-resident murine precursor T cells. *Mol. Immunol.* 34:453–462.
58. Perumal, N.B., T.W. Kenniston, Jr., D.J. Tweardy, K.F. Dyer, R. Hoffman, J. Peschon, and P.M. Appasamy. 1997. TCR-γ genes are rearranged but not transcribed in IL-7Rα-deficient mice. *J. Immunol.* 158:5744–5750.
59. Malissen, M., P. Pereira, D.J. Gerber, B. Malissen, and J.P. DiSanto. 1997. The common cytokine receptor γ chain controls survival of γ/δ T cells. *J. Exp. Med.* 186:1277–1285.
60. Eynon, E.E., F. Livak, K. Kuida, D. Schatz, and R.A. Flavell. 1999. Distinct effects of Jak3 signaling on αβ and γδ thymocyte development. *J. Immunol.* 162:1448–1459.
61. Ye, S.-K., K. Maki, T. Kitamura, S. Sunaga, K. Akashi, J. Domen, I.L. Weissman, T. Honjo, and K. Ikuta. 1999. In-

duction of germline transcription in the TCRγ locus by stat5: implications for accessibility control by the IL-7 receptor. *Immunity*. 11:213–223.
62. Kang, J., M. Coles, and D.H. Raulet. 1999. Defective development of γ/δ T cells in interleukin 7 receptor–deficient mice is due to impaired expression of T cell receptor γ genes. *J. Exp. Med*. 190:973–982.
63. Lefrançois, L., and S. Olson. 1994. A novel pathway of thymus-directed T lymphocyte maturation. *J. Immunol*. 153: 987–995.
64. Wiles, M.V., P. Ruiz, and B.A. Imhof. 1992. Interleukin-7 expression during mouse thymus development. *Eur. J. Immunol*. 22:1037–1042.
65. Huang, E.J., K.H. Nocka, J. Buck, and P. Besmer. 1992. Differential expression and processing of two cell associated forms of the kit-ligand: KL1 and KL-2. *Mol. Biol. Cell*. 3:349–362.
66. Moore, N.C., G. Anderson, C.A. Smith, J.J.T. Owen, and E.J. Jenkinson. 1993. Analysis of cytokine gene expression in subpopulations of freshly isolated thymocytes and thymic stromal cells using semiquantitative polymerase chain reaction. *Eur. J. Immunol*. 23:922–927.
67. Adachi, S., H. Yoshida, K. Honda, K. Maki, K. Saijo, K. Ikuta, T. Saito, and S.-I. Nishikawa. 1998. Essential role of IL-7 receptor α in the formation of Peyer's patch anlage. *Int. Immunol*. 10:1–6.
68. Vajdy, M., M.H. Kosco-Vilbois, M. Kopf, G. Kohler, and N. Lycke. 1995. Impaired mucosal immune responses in interleukin 4–targeted mice. *J. Exp. Med*. 181:41–53.
69. Reynaud, C.A., C.R. Mackay, R.G. Muller, and J.-C. Weill. 1991. Somatic generation of diversity in a mammalian primary lymphoid organ: the sheep ileal Peyer's patches. *Cell*. 64:995–1005.
70. Hertz, M., and D. Nemazee. 1998. Receptor editing and commitment in B lymphocytes. *Curr. Opin. Immunol*. 10: 208–213.
71. Roberts, C.W., J.R. Shutter, and S.J. Korsmeyer. 1994. *Hox11* controls the genesis of the spleen. *Nature*. 368:747–749.
72. Karrer, U., A. Althage, B. Odermatt, C.W. Roberts, S.J. Korsmeyer, S. Miyawaki, H. Hengartner, and R.M. Zinkernagel. 1997. On the key role of secondary lymphoid organs in antiviral immune responses studied in alymphoplastic (*aly/aly*) and spleenless (*Hox11*$^{-/-}$) mutant mice. *J. Exp. Med*. 185:2157–2170.
73. Yoshida, H., K. Honda, R. Shinkura, S. Adachi, S. Nishikawa, K. Maki, K. Ikuta, and S.-I. Nishikawa. 1999. IL-7 receptor α+ CD3− cells in the embryonic intestine induces the organizing center of Peyer's patches. *Int. Immunol*. 11: 643–655.
74. Hardy, R.R., C.E. Carmack, S.A. Shinton, J.D. Kemp, and K. Hayakawa. 1991. Resolution and characterization of pro-B and pre-B cell stages in normal mouse bone marrow. *J. Exp. Med*. 173:1213–1225.